Nickel Catalysis Hot Paper

How to cite:
International Edition: doi.org/10.1002/anie.202106356
German Edition: doi.org/10.1002/ange.202106356

Activation of Aryl Carboxylic Acids by Diboron Reagents towards Nickel-Catalyzed Direct Decarbonylative Borylation

Xi Deng, Jiandong Guo, Xiaofeng Zhang, Xiaotai Wang, and Weiping Su**

Abstract: *The Ni-catalyzed decarbonylative borylation of (hetero)aryl carboxylic acids with B_2cat_2 has been achieved without recourse to any additives. This Ni-catalyzed method exhibits a broad substrate scope covering poorly reactive non-ortho-substituted (hetero)aryl carboxylic acids, and tolerates diverse functional groups including some of the groups active to Ni^0 catalysts. The key to achieve this decarbonylative borylation reaction is the choice of B_2cat_2 as a coupling partner that not only acts as a borylating reagent, but also chemoselectively activates aryl carboxylic acids towards oxidative addition of their C(acyl)−O bond to Ni^0 catalyst via the formation of acyloxyboron compounds. A combination of experimental and computational studies reveals a detailed plausible mechanism for this reaction system, which involves a hitherto unknown concerted decarbonylation and reductive elimination step that generates the aryl boronic ester product. This mode of boron-promoted carboxylic acid activation is also applicable to other types of reactions.*

Introduction

Carboxylic acids are readily available in great structural diversity from both natural and synthetic sources, thus making them attractive starting materials for organic syntheses. The development of catalytic methods for efficient transformations of carboxylic acids into valuable compounds via selective activation of carboxyl group is essential to achieve the potential utility of carboxylic acids as versatile building blocks. In this context, metal-catalyzed decarboxylative cross-coupling reactions of (hetero)aryl carboxylic acids have been explored extensively[1] since seminal work on the reactions of this type[2] and identification of the roles silver or copper salts play in the decarboxylative metalation of (hetero)aryl carboxylic acids,[3] which has led to establishment of a diverse variety of decarboxylative cross-coupling reactions.[1e,f] In spite of the notable progress in this area, such decarboxylative cross-couplings are generally limited to *ortho*-substituted (hetero)aryl carboxylic acids, probably because the existing modes for redox-neutral metal-mediated decarboxylation require *ortho*-substituents to decrease the reaction activation barrier.[4] The oxidative decarboxylation strategy enables non-*ortho*-substituted (hetero)aryl carboxylic acids to participate in decarboxylative functionalization.[5] Nevertheless, thus far, this oxidative decarboxylation strategy has only applied to protodecarboxylation,[5a] decarboxylative halogenation[5d,e] and decarboxylative arylation reactions[5b,c] presumably due to the difficulty in generating thermodynamically unstable aryl radicals, contrasting with its successful applications to the decarboxylative cross coupling-reactions of alkyl carboxylic acids.[6]

Recently, the decarbonylative or decarboxylative cross-coupling reactions of carboxylic acid derivatives have appeared as a powerful tool for formations of C−C and C-heteroatom bonds, opening up a new avenue to expanding synthetic application of abundant carboxylic acids as starting materials.[7–12] Among these established decarbonylative cross-coupling reactions, the decarbonylative borylation reaction of both (hetero)aryl and alkyl carboxylic acid derivatives (e.g. ester, anhydride, amides, and aroyl halides) with diboron compounds as borylating reagents is one of the most extensively explored reactions,[11,12] which was driven by the great importance of organoboron compounds as versatile reagents in synthesis chemistry.[13] As disclosed by these elegant studies, the decarbonylative functionalization reactions benefit from the enhanced redox reactivities of carboxylic acid derivatives towards the oxidative addition to low-valent metal species or single electron transfer redox process. Comparison between carboxylic acids and corresponding carboxylic acid derivatives elucidates that the enhanced redox reactivities of carboxylic acid derivatives structurally result from the bonds between acyl groups and electron-withdrawing groups, namely RC(O)-X bonds (X = halide, OR or NR_2).

Our interest in the metal-catalyzed decarboxylative cross-coupling reactions[5c,14] prompted us to seek after new modes of activation of (hetero)aryl carboxylic acids, hopefully providing a solution to the problem associated with the conventional limitation of substrate scope to *ortho*-substituted (hetero)aryl carboxylic acids, and discovering new types of decarboxylative functionalization reactions. The seminal

[*] X. Deng, Dr. X. Zhang, Prof. Dr. W. Su
State Key Laboratory of Structural Chemistry, Center for Excellence in Molecular Synthesis, Fujian Institute of Research on the Structure of Matter, Chinese Academy of Sciences
Yangqiao West Road 155, Fuzhou 350002 (P. R. China)
E-mail: wpsu@fjirsm.ac.cn
Dr. J. Guo, Prof. Dr. X. Wang
Hoffmann Institute of Advanced Materials, Postdoctoral Innovation Practice Base, Shenzhen Polytechnic
7098 Liuxian Boulevard, Nanshan District, Shenzhen 518055 (P. R. China)
E-mail: xiaotai.wang@ucdenver.edu
Prof. Dr. X. Wang
Department of Chemistry, University of Colorado Denver
Campus Box 194, P. O. Box 173364, Denver, CO 80217-3364 (USA)
X. Deng, Prof. Dr. W. Su
University of Chinese Academy of Sciences
Beijing 100049 (P. R. China)
Supporting information and the ORCID identification number(s) for the author(s) of this article can be found under: https://doi.org/10.1002/anie.202106356.

studies on boron-catalyzed electrophilic reactions of carboxylic acids have disclosed that the electrophilic activation of carboxylic acids by boron catalysts is attributed to formation of acyloxyboron intermediate.[15] The B-O Lewis acid-base interactions have proved to be beneficial to activation of C–O bonds in aryl ether, phenol and allylic alcohol towards oxidation addition to low-valent metal catalyst species.[16] Inspired by these pioneering studies, we questioned whether boron (sp^2) compounds could activate (hetero)aryl carboxylic acids towards oxidative addition of their C(acyl)–O bonds to low-valent metal catalyst through formation of acyloxyboron species, which would trigger decarbonylation and subsequent coupling step. Herein, we demonstrate that this assumed mode of boron-promoted carboxylic acid activation is viable, report a direct decarbonylative borylation reaction of (hetero)aryl carboxylic acids with bis(catecholato)diboron (B_2cat_2) that is catalyzed by a Ni/dcypm catalyst (dcypm = bis(dicyclohexylphosphino)methane) and proceeds without recourse to any additive (Scheme 1). The key to achieve this Ni-catalyzed direct decarbonylative borylation is our discovery of B_2cat_2 as a proper diboron reagent that acted not only as a borylating reagent/coupling partner, but also as an activator of (hetero)aryl carboxylic acids. This protocol eliminates the need for stoichiometric transition metal salts that mediate decarboxylation and/or serve as terminal oxidants in the previously developed decarboxylative cross-coupling reactions, avoids in situ generation of activated aryl carboxylic acid derivatives from the corresponding acids, while enabling a broad range of (hetero)aryl carboxylic acids including normally poorly reactive non-*ortho*-substituted carboxylic acids[1,2] to be coupled.

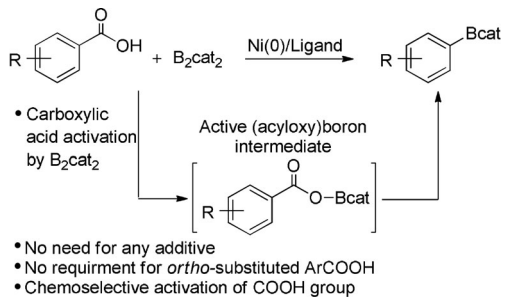

Scheme 1. Boron-promoted activation of aryl carboxylic acids towards directd decarbonylative borylation.

Results and Discussion

Reaction Optimization

We began our investigation by studying the borylation of 4-phenylbenzoic acid (**1b**) with B_2cat_2 (**2**) as a model reaction (Table 1). After screening a variety of reaction conditions, we determined that a combination of $Ni(COD)_2$ (10 mol%), dcypm (20 mol%), B_2cat_2 (2.0 equiv), and **1b** (0.2 M) in toluene at 150 °C delivered the desired coupling product in the best yield after 24 h of reaction (entry 1). Note that the catechol arylboronate product **3b** was-without isolation-treated with pinacol and Et_3N to convert to the more stable

Table 1: Optimization Studies on Decarbonylative Borylation of Aryl Carboxylic Acids.[a]

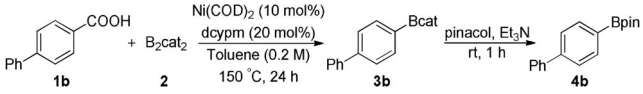

Entry	Variation from the standard conditions	Yield of **4b**[b] [%]
1	none	76 (71[c])
2	10 mol% dcypm	52
3	10 mol% dcype instead of dcypm	15
4	10 mol% dcypp instead of dcypm	21
5	20 mol% PCy_3 instead of dcypm	23
6	10 mol% dppm instead of dcypm	<10
7	2.0 equiv B_2pin_2 instead of B_2cat_2	NA
8	adding 0.2 equiv KOAc	50
9	1.0 mL DMSO instead of toluene	<5
10	1.0 mL Dioxane instead of toluene	18
11	130 °C instead of 150 °C	30

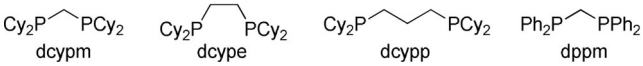

[a] All reactions were run with **1b** (0.2 mmol) and **2** (0.4 mmol) in 1 mL toluene solution containing $Ni(COD)_2$/dcypm under N_2, followed by treatment with pinacol (0.8 mmol) and Et_3N (0.4 mL) at room temperature for 1 h. [b] Yield determined by GC analysis with *n*-dodecane as the internal standard. [c] Yield of isolated **4b**.

pinacol arylboronate product **4b** in 76% and 71% GC and isolated yields, respectively. Phosphine ligands and their loading were observed to have a profound effect on the reaction outcomes. Decreasing loading of dcypm to 10 mol% brought about a drop in yield to 52% (entry 2). In contrast to dcypm, bidentate ligands capable of forming stable five- or six-membered chelate ring, namely dcype and dcypp (10 mol%), and monodentate PCy_3 (20 mol%) were much less effective (entries 3, 4 and 5), although these ligands are known to promote the Ni-catalyzed decarbonylative cross-coupling reactions of benzoic acid derivatives.[8b,e] Less electron-donating dppm ligand was far interior to dcypm, despite its structural similarity to dcypm (entry 6). Intriguingly, when bis(pinacolato)diboron (B_2pin_2) was used in place of B_2cat_2, no reaction took place, with essentially all of B_2pin_2 recovered (entry 7), indicating a difference between B_2cat_2 and B_2pin_2 in terms of reactivity with aryl carboxylic acids. Addition of sub-stoichiometric bases (0.2 equiv), such as KOAc, proved to be detrimental to the reaction (entry 8), although such base additives are frequently used to promote transmetalation in transition metal-catalyzed cross-coupling reactions of boron reagents.[11g] Similarly to the effect of external bases, coordinating solvents such as DMSO and 1,4-dioxane either shut down the reaction or gave much lower yields than toluene (entries 9 and 10). Attempt to conduct reaction at lower temperature failed to give a satisfied yield (entry 11).

Evaluation of Substrate Scope

With the optimized reaction conditions in hand, we further evaluated generality of this decarbonylative borylation (Scheme 2).[17] To obtain consistent isolated yields, all

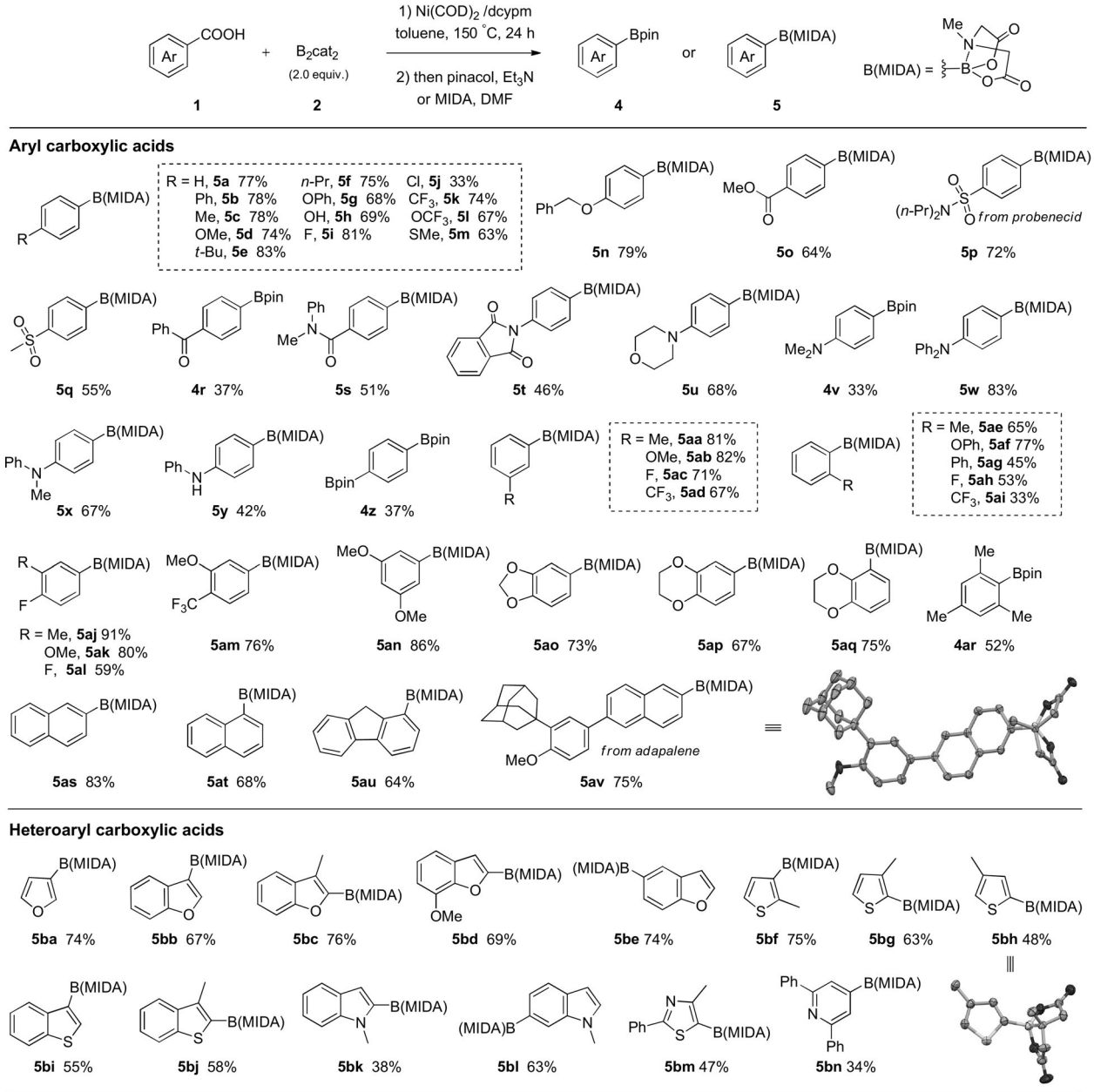

Scheme 2. Substrate scope for Ni-catalyzed direct decarbonylative borylation of (hetero)aryl carboxylic acids.[a] [a]All reactions were run with 1 (0.2 mmol), 2 (0.4 mmol), $Ni(COD)_2$ (10 mol%), dcypm (20 mol%) in 1 mL toluene for 24 h at 150°C under N_2 and then treated with pinacol (0.8 mmol) and Et_3N (0.4 mL) at room temperature for 1 h or with MIDA (0.8 mmol) and DMF (2 mL) at 90°C for 4 h. Yields of isolated products are reported.

catechol arylboronate products **3** were converted through ligand exchange to the more air- and moisture-stable pinacol arylboronate products **4** or N-methyliminodiacetic acid (MIDA)-protected arylboronates **5** for isolation and yield determination.[18] Monosubstituted benzoic acids bearing electronically diverse substituents in the *para*- or *meta*-position reacted to form the corresponding arylboronate esters **5b**–**5q**, **4r**, **5s**–**5u**, **4v**, **5w**–**5y**, **4z**, and **5aa**–**5ad** in fair to excellent yields. *Ortho*-monosubstituted benzoic acids, despite being somewhat sterically hindered, also reacted effectively, producing **5ae**–**5ai** in yields ranging from 33 to 77%. Many disubstituted benzoic acids were attempted, which afforded the corresponding disubstituted arylboronate esters **5aj**–**5aq** in generally good yields. Trisubstituted 2,4,6-trimethylbenzoic acid performed well, affording the mesitylboronate ester **4ar** in 52% yield. Polycyclic aromatic acids exhibited high levels of reactivity in this protocol, as shown by the formation of the polycyclic arylboronate esters **5as**–**5av**.

Heteroaryl carboxylic acids, akin to their halide congeners, are abundant, inexpensive, and stable compounds. Under our standard reaction conditions, a variety of heteroaryl carboxylic acids, including (benzo)furan, (benzo)thiophene, indole, and thiazole derivatives, were converted to the

corresponding heteroaryl boronate esters **5ba**–**5bm** in good yields. Isonicotinic acid, a simple pyridine-derivatized carboxylic acid, did not work for the decarbonylative borylation, but 2,6-diphenyl isonicotinic acid could afford the boronate ester **5bn** in a moderate yield. These results suggest that the pyridinyl group might react with the diboron reagent to interfere with the carboxyl activation but that the reaction might be stalled by the steric hindrance of the two N-adjacent phenyl substituents in 2,6-diphenyl isonicotinic acid.

In summary, a broad range of aryl carboxylic acids, which bear electronically and sterically diverse functional groups, such as ether, thioether, hydroxy, fluoro, chloro, ester, ketone, amide, sulfonamide, and pinacol boronate, were compatible with our decarbonylative borylation protocol. Thus, the protocol demonstrates a potential utility in iterative cross-coupling reactions. Particularly, alkyloxy,[19a–c] fluoro,[19d–g] and amide groups,[19h] which are effective leaving groups in an array of Ni-catalyzed cross-coupling reactions with diboron reagents, were perfectly tolerated, illustrating that our method is orthogonal to those Ni-catalyzed reactions. It is worth noting that two carboxylic acid-based pharmaceuticals, namely probenecid and adapalene, were transformed into the borylated products **5p** and **5av** in moderate to high yields. This is a further demonstration that the protocol could be useful for the elaboration of bioactive compounds. It should be noted that benzoic acids bearing a strongly electron-withdrawing nitro or cyano group does not perform well for this decarbonylative borylation protocol, presumably because such groups significantly decrease the affinity of the carboxyl group for the Lewis-acidic diboron reagent.

The strategy of activating carboxylic acids with boron reagents could also be exploited in the decarbonylative borylation of aryl carboxylic acid anhydrides and the direct conversion of alky carboxylic acids into olefins,[20] as shown in Scheme S1.

Mechanistic Studies

We employed a combination of experiments and DFT calculations to gain insight into the mechanism of the new catalytic reaction. In the execution of the model reaction of 4-phenylbenzoic acid (**1b**) with B_2cat_2, we observed H_2 and CO in the gas phase by GC, thereby confirming the decarbonylative nature of the reaction (Figure S1). ^{11}B NMR measurements were carried out to monitor the reactions of benzoic acid (**1a**) with B_2cat_2 and related boron reagents (Scheme 4). A previous ^{11}B NMR study by Antilla et al. on the reaction of a phosphoric acid with catecholborane (HBcat) provided useful reference,[21] which showed release of H_2 gas and formation of a new phosphoryloxyboron species with a distinct ^{11}B NMR peak at 22.1 ppm [Scheme 3, Eq. (1)]. In analyzing the reaction of benzoic acid with HBcat, we observed gas evolution and a major ^{11}B NMR peak at 21.8 ppm [Scheme 3, Eq. (2)], which was assigned to an aroyloxyboron species by analogy to Antilla's work (Figure S2). In addition, a minor peak appeared at 3.1 ppm and would grow in size as the amount of benzoic acid was increased. We assign the 3.1 ppm peak to a benzoic acid-

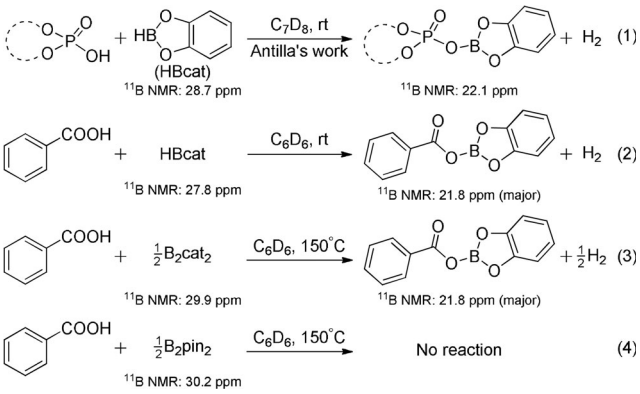

Scheme 3. Reactivity of boron reagents with benzoic acid.[a] [a] See Figure S2 for the NMR spectra.

aroyloxyboron complex containing a four-coordinate boron center which is known to give a ^{11}B NMR chemical shift in that region of the spectrum (Figure S2).[22] Moreover, the aroyloxyboron species generated from the reaction of B_2cat_2 with benzoic acid could be isolated in the form of $ArCOOBcat{\cdot}(ArCOO)_2Ni$ adduct and structurally characterized by single crystal X-ray diffraction analysis (Figure S3)[17] when the reaction solution of B_2cat_2 with benzoic acid was treated with 0.5 equiv of Ni^{II} carboxylate salt.

To our delight, the reaction of benzoic acid with half an equivalent of B_2cat_2 under heating [Scheme 3, Eq. (3)] showed exactly the same ^{11}B and ^{1}H NMR results as the reaction of benzoic acid with HBcat, indicating that B_2cat_2 could activate aryl carboxylic acids to form aroyloxyborons at elevated temperatures (Figure S2). This control experiment lends support to the idea that B_2cat_2 plays a dual role in our reaction as a carboxylic acid activator and a coupling partner. In contrast, no reaction was detected for a mixture of benzoic acid and B_2pin_2 under the same conditions [Scheme 3, Eq. (4)], suggesting that B_2pin_2 could not activate aryl carboxylic acids even at elevated temperatures. This result agrees with the observation that B_2pin_2 is an ineffective diboron reagent for the cross-coupling reaction (Table 1, entry 7).

To establish a detailed plausible mechanism for the title reaction, we carried out extensive density functional theory (DFT) calculations on the reaction of benzoic acid (**1a**) beginning with its activation by B_2cat_2. As shown in Figure 1, benzoic acid reacts with B_2cat_2 by concerted metathesis via the six-membered transition state **TS1**, wherein the O–H and B–B bonds are breaking by heterolysis and the B–O and H–B bonds are forming through Lewis acid-base interaction. **TS1** proceeds to HBcat with the release of the aroyloxyboron species PhCOOBcat. HBcat continues to react with **1a** by concerted metathesis via the five-membered **TS2** to form PhCOOBcat and release H_2 gas. Thermodynamically this activation process is favorable ($\Delta G = -34.4$ kcal mol^{-1}), and kinetically it has the highest energy barrier of 33.5 kcal mol^{-1} (B_2cat_2 to **TS1**).[23] We also computed the mechanism of the reaction of benzoic acid with B_2pin_2, for which the energy barrier **TS1′** is higher than **TS1** by 1.6 kcal mol^{-1} (Figure S4). As estimated by using the Eyring equation, the reaction of

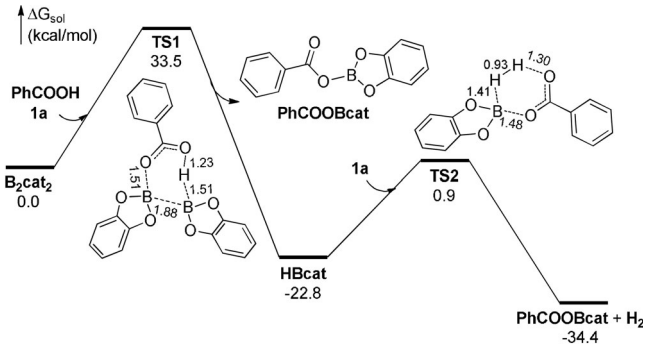

Figure 1. Free energy profile for the activation of benzoic acid by B_2cat_2 computed with M06/BS2//B3LYP/BS1 (the same below; see Computational Methods in the Supporting Information). Selected bond distances are given in Å (the same below).

benzoic acid with B_2pin_2 would be 15 times slower than the reaction with B_2cat_2 under the same conditions. These calculations are qualitatively consistent with the experimental findings. Conceptually, the reactivity difference between B_2cat_2 and B_2pin_2 can be understood by considering that B_2pin_2 is a weaker Lewis acid than B_2cat_2. Benchmark calculations on **TS1** and **TS1′** at a higher level of theory gave consistent and more accurate results (Figure S5).

The next phase of reaction is the oxidative addition of PhCOOBcat to Ni^0 (Figure 2). The precatalyst $Ni(COD)_2$ is

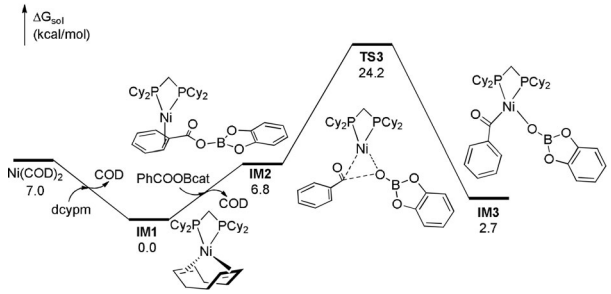

Figure 2. Free energy profile for the PhCOOBcat to Ni^0 oxidative addition.

activated by reacting with the ancillary diphosphine ligand dcypm, for which we have considered various products (Figure S6). **IM1** is the most stable species generated, and the initiation process is thermodynamically favorable by 7.0 kcal mol^{-1}. **IM1** takes up PhCOOBcat by substituting it for COD to form the precursor complex **IM2**, which undergoes subsequent intramolecular oxidative addition involving the PhC(O)-OBcat bond cleavage via the transition state **TS3**, which proceeds to the square planar Ni^{II} d^8 complex **IM3** bearing a benzoyl ligand. The oxidative addition has an overall activation barrier of 24.2 kcal mol^{-1} (**IM1** to **TS3**) in the initial catalytic cycle. We also considered and ruled out the alternative oxidative addition involving the Ph-COOBcat bond cleavage, which would have a significantly higher barrier than **TS3** (Figure S7).

Pathways of direct transmetalation of **IM3** with B_2cat_2 through five-coordinate intermediates/transition states could not be found due to the steric hindrance around the four-coordinate Ni^{II} center. Dissociation of one phosphine arm via **TS4** converts **IM3** into the three-coordinate **IM4**, which subsequently combines with B_2cat_2 to give **IM5**. This four-coordinate intermediate launches intramolecular transmetalation involving heterolytic B–B bond cleavage via the four-membered transition state **TS5**, which delivers the dioxaborolyl (boryl hereafter) group to the Ni^{II} center in **IM6** and releases the byproduct catBOBcat (Figure S8). Rebound of the second dangling phosphine arm in **IM6** converts it into the much more stable four-coordinate complex **IM7**.

No transition state of decarbonylation/phenyl migration from **IM7** could be found probably because of the large space separating the phenyl group and the Ni^{II} center. We traced the interchange transition state **TS6** connecting from **IM7** and proceeding to **IM8** with the opening of the diphosphine chelate ring. The geometry of the η^2-π complex **IM8** is such that it brings the Ni^{II} center and the phenyl group into a proper spatial relationship.This symphoria facilitates the decarbonylation/phenyl migration via **TS7**, which would be expected to proceed to a square planar Ni^{II} carbonyl intermediate bearing a phenyl cis to the boryl group. Such a structure was indeed observed along the calculated intrinsic reaction coordinate (IRC) of **TS7** (Figure S9) but could not be optimized as an energy minimum; it transforms downhill into **IM9**, a Ni^0 complex bearing the reductive elimination (or phenyl-boryl coupling) product PhBcat. As a benchmark study, we reoptimized **TS7** using three other density functionals, i.e., M06-L, wB97XD, and X3LYP, and the computed transition states all behave like **TS7** and proceed to **IM9** (Figure S10). Thus, the calculations strongly suggest a concerted process of decarbonylation (or phenyl migration to nickel) and reductive elimination of the phenyl-boryl coupling product. This could be explained by considering the significant natural charges on the boron (+0.80) and *ipso*-carbon (−0.23) atoms in **TS7**, which show a tendency of phenyl-boryl interaction when the two groups become close to each other. This concerted decarbonylation and reductive elimination mechanism (**IM8** → **IM9** via **TS7**) has not been known before, and the closest analogy was seen in a computational study of copper-catalyzed borylation, which involves the concerted PhI to Cu^I oxidative addition and reductive phenyl-boryl elimination/coupling.[24] In addition, concerted β-hydrogen elimination and reductive hydrogen-vinyl elimination/coupling pathways were found by a number of computational studies on nickel-catalyzed reactions.[25]

Rebound of the open phosphine arm in **IM9** converts it into **IM10**, which extrudes CO via the dissociative transition state **TS8** to form **IM11**. Substitution of COD by **IM11** releases the borylation product PhBcat, regenerates the active species **IM1**, and closes the catalytic cycle. Thus, a detailed plausible mechanism for the title reaction has now been established computationally. It reveals a complex yet well-defined reaction system consisting of two portions: (a) the activation of aryl carboxylic acids by B_2cat_2 (Figure 1) and (b) the catalytic cycle beginning with the active species **IM1** (Figure 2, Figure 3, and Figure 4). The balanced equations for the two portions and the overall reaction are the following:

$$\mathrm{PhCOOH} + \frac{1}{2}\mathrm{B_2cat_2} \rightarrow \mathrm{PhCOOBcat} + \frac{1}{2}\mathrm{H_2} \quad (1a)$$

$$\mathrm{PhCOOBcat} + \mathrm{B_2cat_2} \rightarrow \mathrm{PhBcat} + \mathrm{catBOBcat} + \mathrm{CO} \quad (1b)$$

$$\mathrm{PhCOOH} + \frac{3}{2}\mathrm{B_2cat_2} \rightarrow \mathrm{PhBcat} + \mathrm{catBOBcat} + \mathrm{CO} + \frac{1}{2}\mathrm{H_2} \quad (1c)$$

The activation of benzoic acid by B_2cat_2 has a barrier of 33.5 kcal mol^{-1} that is consistent with the reaction temperature (150 °C),[11f,26] and the resulting borolyl benzoate PhCOOBcat enters the catalytic cycle by replacing COD from **IM1** (Figure 2). The largest energy span in the initial catalytic cycle is from **IM7** to **TS7**, 24.4 kcal mol^{-1} (Figure 4). Because **IM9** is lower in energy than the regenerated active catalyst **IM1** by 8.7 kcal mol^{-1} (Figure 4), beginning with the second catalytic cycle, **IM9** should be the reference state of the oxidative addition barrier **TS3** (Figure 2), which causes **TS3** to be 32.9 kcal mol^{-1} (24.2 + 8.7) and hence the turnover-limiting barrier. This overall activation barrier is also consistent with the reaction temperature (150 °C).[11f,26] The catalytic cycle has a large thermodynamic driving force ($\Delta G = -35.0$ kcal mol^{-1}). Although the segment from **IM9** through **IM1** is endergonic by 8.7 kcal mol^{-1} (Figure 4), **IM9** would not cause a thermodynamic sink on the reaction coordinate, because the extrusion of CO gas from **IM10** shifts the equilibrium position forward. We also considered an alternative route in which decarbonylation (from **IM4**) would precede transmetalation; this pathway could be ruled out because it would lead to a concerted transmetalation and reductive elimination with a very high-energy barrier, **TS12** (Figure S11).

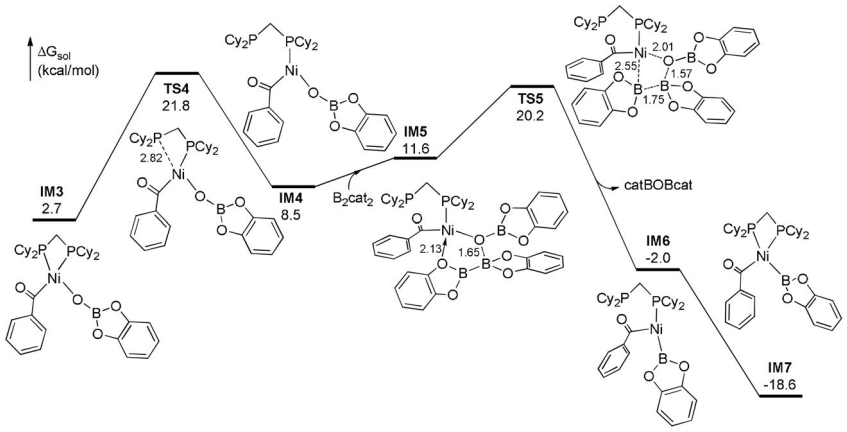

Figure 3. Free energy profile for the transmetalation with B_2cat_2.

Conclusion

We have developed a Ni-catalyzed method that enables the direct decarbonylative borylation of (hetero)aryl carboxylic acids without recourse to any additive. This method is applicable to a broad range of (hetero)aryl carboxylic acids including normally poorly reactive non-*ortho*-substituted acids, demonstrates a good chemoselectivity for carboxyl group over some of the groups active to electron-rich Ni^0 catalysts. The choice of B_2cat_2 is crucial to the success of the catalytic protocol. This diboron reagent not only serves as the borylating agent, it also activates the carboxylic acid to form the aroyloxyboron for oxidative addition to Ni^0 involving the ArC(O)-OBcat bond cleavage. A combination of experiments and extensive DFT calculations reveals a detailed plausible mechanism, the key aspects of which are recapitulated in Scheme 4. The active Ni^0 species **IM1** reacts with the aroyloxyboron by oxidative addition, and the resulting Ni^{II} complex **IM3** undergoes single phosphine dissociation to **IM4**, followed by transmetalation with B_2cat_2, to deliver the boryl group to the Ni^{II} center in **IM6** *or* **IM8**, a cis-Ni^{II}(aroyl)(boryl) complex. The reaction then proceeds by an unprecedented concerted decarbonylation and reductive elimination mechanism via **TS7** to afford the carbonyl complex **IM9** bearing the aryl boronic ester product. Subsequent phosphine rebound enables CO dissociation from **IM10**, which is followed by COD substitution to release the product and regenerate the active species **IM1**. Further

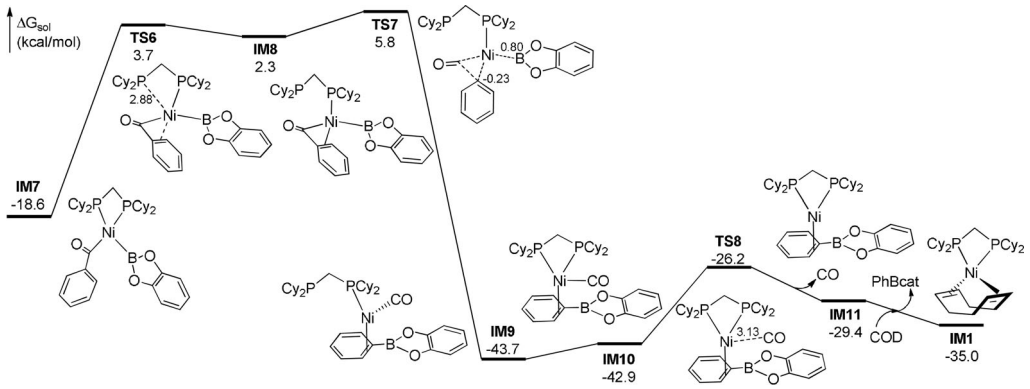

Figure 4. Free energy profile for the concerted decarbonylation and reductive elimination, followed by catalyst regeneration. The numbers denote natural charges on selected atoms in **TS7**.

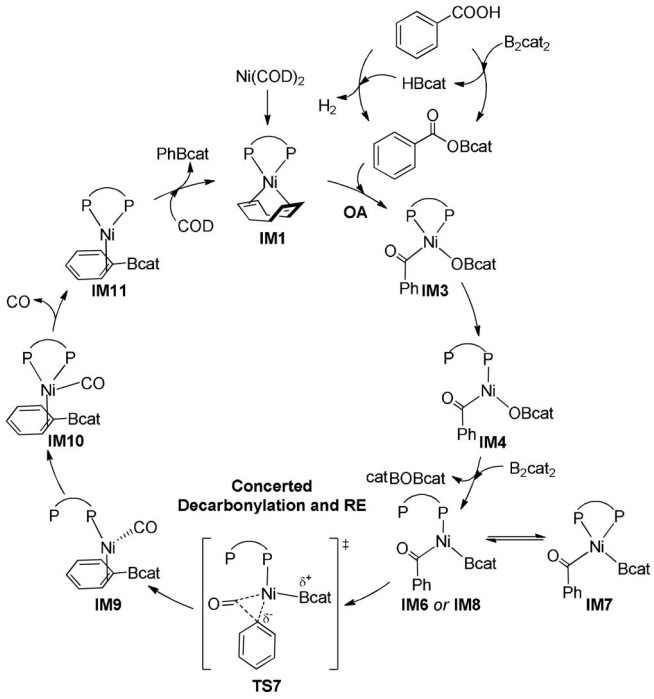

Scheme 4. Summary of mechanism of Ni-catalyzed direct decarbonylative borylation of aryl carboxylic acids.

efforts are underway to leverage the mode of boron activating carboxylic acids to develop new direct cross-coupling reactions of carboxylic acids.

Acknowledgements

This work is supported by the National Key Research and Development Program of China (2018YFA0704502), the National Natural Science Foundation of China Grant (21931011, 22071241, 22071243), the Key Research Program of Frontier Sciences of the Chinese Academy of Sciences (QYZDJ-SSW-SLH024), and the Strategic Priority Research Program of the Chinese Academy of Science (XDB20000000). X.W. acknowledges support from the Hoffmann Institute of Advanced Materials, Shenzhen Polytechnic and the University of Colorado Denver.

Conflict of Interest

The authors declare no conflict of interest.

Keywords: borylation · carboxylic acid activation · decarbonylative cross-coupling · DFT studies · nickel catalysis

[1] The reviews on decarboxylative cross-coupling reactions of aryl carboxylic acids, see: a) L. J. Goossen, N. Rodríguez, K. Goossen, *Angew. Chem. Int. Ed.* **2008**, *47*, 3100 – 3120; *Angew. Chem.* **2008**, *120*, 3144 – 3164; b) N. Rodríguez, L. J. Goossen, *J. Chem. Soc. Rev.* **2011**, *40*, 5030 – 5048; c) R. Shang, L. Liu, *Sci. China Chem.* **2011**, *54*, 1670 – 1687; d) I. Larrosa, J. Cornella, *Synthesis* **2012**, *44*, 653; e) G. J. P. Perry, I. Larrosa, *Eur. J. Org. Chem.* **2017**, 3517 – 3527; f) Y. Wei, P. Hu, M. Zhang, W. Su, *Chem. Rev.* **2017**, *117*, 8864 – 8907.

[2] a) A. G. Myers, D. Tanaka, M. R. Mannion, *J. Am. Chem. Soc.* **2002**, *124*, 11250 – 11251; b) L. J. Goossen, G. Deng, L. M. Levy, *Science* **2006**, *313*, 662 – 664; c) A. Voutchkova, A. Coplin, N. E. Leadbeater, R. H. Crabtree, *Chem. Commun.* **2008**, *47*, 6312 – 6314; d) C. Wang, I. Piel, F. Glorius, *J. Am. Chem. Soc.* **2009**, *131*, 4194 – 4195; e) M. Miyasaka, A. Fukushima, T. Satoh, K. Hirano, M. Miura, *Chem. Eur. J.* **2009**, *15*, 3674 – 3677; f) J. Cornella, P. Lu, I. Larrosa, *Org. Lett.* **2009**, *11*, 5506 – 5509; g) F. Zhang, M. F. Greaney, *Angew. Chem. Int. Ed.* **2010**, *49*, 2768 – 2771; *Angew. Chem.* **2010**, *122*, 2828 – 2831.

[3] a) L. J. Goossen, C. Linder, N. Rodríguez, P. P. Lange, A. Fromm, *Chem. Commun.* **2009**, 7173 – 7175; b) J. Cornella, C. Sanchez, D. Banawa, I. Larrosa, *Chem. Commun.* **2009**, 7176 – 7178.

[4] a) L. Xue, W. Su, Z. Lin, *Dalton Trans.* **2011**, *40*, 11926 – 11936; b) R. Grainger, J. Cornella, D. C. Blakemore, I. Larrosa, J. M. Campanera, *Chem. Eur. J.* **2014**, *20*, 16680 – 16687.

[5] a) S. Seo, J. B. Taylor, M. F. Greaney, *Chem. Commun.* **2012**, *48*, 8270 – 8272; b) S. Seo, M. Slater, M. F. Greaney, *Org. Lett.* **2012**, *14*, 2650 – 2653; c) J. Kan, S. Huang, J. Lin, M. Zhang, W. Su, *Angew. Chem. Int. Ed.* **2015**, *54*, 2199 – 2203; *Angew. Chem.* **2015**, *127*, 2227 – 2231; d) L. Candish, M. Freitag, T. Gensch, F. Glorius, *Chem. Sci.* **2017**, *8*, 3618 – 3622; e) G. J. P. Perry, J. M. Quibell, A. Panigrahi, I. Larrosa, *J. Am. Chem. Soc.* **2017**, *139*, 11527 – 11536.

[6] The selected examples of oxidative decarboxylation cross-coupling reactions of alkyl carboxylic acids, see: a) X. Liu, Z. Wang, X. Cheng, C. Li, *J. Am. Chem. Soc.* **2012**, *134*, 14330 – 14333; b) A. Noble, S. J. McCarver, D. W. C. MacMillan, *J. Am. Chem. Soc.* **2015**, *137*, 624 – 627; c) Q.-Q. Zhou, W. Guo, W. Ding, X. Wu, X. Chen, L.-Q. Lu, W.-J. Xiao, *Angew. Chem. Int. Ed.* **2015**, *54*, 11196 – 11199; *Angew. Chem.* **2015**, *127*, 11348 – 11351; d) Z.-J. Liu, X. Lu, G. Wang, L. Li, W.-T. Jiang, Y.-D. Wang, B. Xiao, Y. Fu, *J. Am. Chem. Soc.* **2016**, *138*, 9714 – 9719.

[7] The recent reviews on decarbonylative cross-coupling reactions of carboxylic acid derivatives, see: a) Z. Wang, X. Wang, Y. Nishihara, *Chem. Asian J.* **2020**, *15*, 1234 – 1247; b) Y. Ogiwara, N. Sakai, *Angew. Chem. Int. Ed.* **2020**, *59*, 574 – 594; *Angew. Chem.* **2020**, *132*, 584 – 605; c) N. Blanchard, V. Bizet, *Angew. Chem. Int. Ed.* **2019**, *58*, 6814 – 6817; *Angew. Chem.* **2019**, *131*, 6886 – 6889; d) L. Guo, M. Rueping, *Acc. Chem. Res.* **2018**, *51*, 1185 – 1195; e) G. Meng, M. Szostak, *Eur. J. Org. Chem.* **2018**, 2352 – 2365; f) R. Takise, K. Muto, J. Yamaguchi, *Chem. Soc. Rev.* **2017**, *46*, 5864 – 5888; g) H. Lu, T.-Y. Yu, P.-F. Xu, H. Wei, *Chem. Rev.* **2021**, *121*, 365 – 411.

[8] a) L. J. Goossen, J. Paetzold, *Angew. Chem. Int. Ed.* **2002**, *41*, 1237 – 1241; *Angew. Chem.* **2002**, *114*, 1285 – 1289; b) K. Muto, J. Yamaguchi, D. G. Musaev, K. Itam, *Nat. Commun.* **2015**, *6*, 7508 – 7510; c) A. Chatupheeraphat, H.-H. Liao, W. Srimontree, L. Guo, Y. Minenkov, A. Poater, L. Cavallo, M. Rueping, *J. Am. Chem. Soc.* **2018**, *140*, 3724 – 3735; d) R. Takise, R. Isshiki, K. Muto, K. Itami, J. Yamaguchi, *J. Am. Chem. Soc.* **2017**, *139*, 3340 – 3343; e) C. A. Malapit, M. Borrell, M. W. Milbauer, C. E. Brigham, M. S. Sanford, *J. Am. Chem. Soc.* **2020**, *142*, 5918 – 5923.

[9] a) M. S. Stephan, A. J. J. M. Teunissen, G. K. M. Verzijl, J. G. de Vries, *Angew. Chem. Int. Ed.* **1998**, *37*, 662 – 664; *Angew. Chem.* **1998**, *110*, 688 – 690; b) F. Pan, Z.-Q. Lei, H. Wang, H. Li, J. Sun, Z.-J. Shi, *Angew. Chem. Int. Ed.* **2013**, *52*, 2063 – 2067; *Angew. Chem.* **2013**, *125*, 2117 – 2121; c) G. Meng, M. Szostak, *Angew. Chem. Int. Ed.* **2015**, *54*, 14518 – 14522; *Angew. Chem.* **2015**, *127*, 14726 – 14730; d) S. Shi, G. Meng, M. Szostak, *Angew. Chem. Int. Ed.* **2016**, *55*, 6959 – 6963; *Angew. Chem.* **2016**, *128*,

7073 – 7077; e) C. A. Malapit, J. R. Bour, C. E. Brigham, M. S. Sanford, *Nature* **2018**, *563*, 100 – 104.

[10] a) K. Okada, K. Okamoto, N. Morita, K. Okubo, M. Oda, *J. Am. Chem. Soc.* **1991**, *113*, 9401 – 9402; b) G. Pratsch, G. L. Lackner, L. E. Overman, *J. Org. Chem.* **2015**, *80*, 6025 – 6036; c) T. Qin, J. Cornella, C. Li, L. R. Malins, J. T. Edwards, S. Kawamura, B. D. Maxwell, M. D. Eastgate, P. S. Baran, *Science* **2016**, *352*, 801 – 805; d) F. Toriyama, J. Cornella, L. Wimmer, T.-G. Chen, D. D. Dixon, G. Creech, P. S. Baran, *J. Am. Chem. Soc.* **2016**, *138*, 11132 – 11135; e) J. Wang, T. Qin, T.-G. Chen, L. Wimmer, J. T. Edwards, J. Cornella, B. Vokits, S. A. Shaw, P. S. Baran, *Angew. Chem. Int. Ed.* **2016**, *55*, 9676 – 9679; *Angew. Chem.* **2016**, *128*, 9828 – 9831; f) K. M. M. Huihui, J. A. Caputo, Z. Melchor, A. M. Olivares, A. M. Spiewak, K. A. Johnson, T. A. DiBenedetto, S. Kim, L. K. G. Ackerman, D. J. Weix, *J. Am. Chem. Soc.* **2016**, *138*, 5016 – 5019; g) X. Liu, J. Jia, M. Rueping, *ACS Catal.* **2017**, *7*, 4491 – 4496; h) J. Masson-Makdissi, J. K. Vandavasi, S. G. Newman, *Org. Lett.* **2018**, *20*, 4094 – 4098; i) T. Patra, P. Bellotti, F. Strieth-Kalthoff, F. Glorius, *Angew. Chem. Int. Ed.* **2020**, *59*, 3172 – 3177; *Angew. Chem.* **2020**, *132*, 3198 – 3203.

[11] a) X. Pu, J. Hu, Y. Zhao, Z. Shi, *ACS Catal.* **2016**, *6*, 6692 – 6698; b) J. Hu, Y. Zhao, J. Liu, Y. Zhang, Z. Shi, *Angew. Chem. Int. Ed.* **2016**, *55*, 8718 – 8722; *Angew. Chem.* **2016**, *128*, 8860 – 8864; c) H. Ochiai, Y. Uetake, T. Niwa, T. Hosoya, *Angew. Chem. Int. Ed.* **2017**, *56*, 2482 – 2486; *Angew. Chem.* **2017**, *129*, 2522 – 2526; d) L. Candish, M. Teders, F. Glorius, *J. Am. Chem. Soc.* **2017**, *139*, 7440 – 7443; e) Z. Wang, X. Wang, Y. Nishihara, *Chem. Commun.* **2018**, *54*, 13969 – 13972; f) C. Liu, C.-L. Ji, X. Hong, M. Szostak, *Angew. Chem. Int. Ed.* **2018**, *57*, 16721 – 16726; *Angew. Chem.* **2018**, *130*, 16963 – 16968; g) C. A. Malapit, J. R. Bour, S. R. Laursen, M. S. Sanford, *J. Am. Chem. Soc.* **2019**, *141*, 17322 – 17330.

[12] a) C. Li, J. Wang, L. M. Barton, S. Yu, M. Tian, D. S. Peters, M. Kumar, A. W. Yu, K. A. Johnson, A. K. Chatterjee, M. Yan, P. S. Baran, *Science* **2017**, *356*, eaam7355; b) A. Fawcett, J. Pradeilles, Y. Wang, T. Mutsuga, E. L. Myers, V. K. Aggarwal, *Science* **2017**, *357*, 283 – 286; c) D. Hu, L. Wang, P. Li, *Org. Lett.* **2017**, *19*, 2770 – 2773.

[13] a) *Boronic acids: preparation and applications in organic synthesis medicine and materials*, 2nd ed. (Ed.: D. G. Hall), Wiley-VCH, Weinheim, **2011**; b) N. Miyaura, A. Suzuki, *Chem. Rev.* **1995**, *95*, 2457 – 2483.

[14] a) J. Zhou, P. Hu, M. Zhang, S. Huang, M. Wang, W. Su, *Chem. Eur. J.* **2010**, *16*, 5876 – 5880; b) P. Hu, M. Zhang, X. Jie, W. Su, *Angew. Chem. Int. Ed.* **2012**, *51*, 227 – 231; *Angew. Chem.* **2012**, *124*, 231 – 235; c) P. Hu, Y. Shang, W. Su, *Angew. Chem. Int. Ed.* **2012**, *51*, 5945 – 5949; *Angew. Chem.* **2012**, *124*, 6047 – 6051; d) Y. Zhang, H. Zhao, M. Zhang, W. Su, *Angew. Chem. Int. Ed.* **2015**, *54*, 3817 – 3821; *Angew. Chem.* **2015**, *127*, 3888 – 3892.

[15] a) K. Ishihara, S. Ohara, H. Yamamoto, *J. Org. Chem.* **1996**, *61*, 4196 – 4197; b) T. Maki, K. Ishiharaa, H. Yamamoto, *Tetrahedron* **2007**, *63*, 8645 – 8657; c) R. M. Al-Zoubi, O. Marion, D. G. Hall, *Angew. Chem. Int. Ed.* **2008**, *47*, 2876 – 2879; *Angew. Chem.* **2008**, *120*, 2918 – 2921; d) H. Zheng, R. McDonald, D. G. Hall, *Chem. Eur. J.* **2010**, *16*, 5454 – 5460; e) H. Charville, D. Jackson, G. Hodges, A. Whiting, *Chem. Commun.* **2010**, *46*, 1813 – 1823; f) Y. Morita, T. Yamamoto, H. Nagai, Y. Shimizu, M. Kanai, *J. Am. Chem. Soc.* **2015**, *137*, 7075 – 7078; g) D. G. Hall, *Chem. Soc. Rev.* **2019**, *48*, 3475 – 3496.

[16] a) Y. Tamaru, Y. Horino, M. Araki, S. Tanaka, M. Kimura, *Tetrahedron Lett.* **2000**, *41*, 5705 – 5709; b) D.-G. Yu, Z.-J. Shi, *Angew. Chem. Int. Ed.* **2011**, *50*, 7097 – 7100; *Angew. Chem.* **2011**, *123*, 7235 – 7238; c) L. Guo, X. Liu, C. Baumann, M. Rueping, *Angew. Chem. Int. Ed.* **2016**, *55*, 15415 – 15419; *Angew. Chem.* **2016**, *128*, 15641 – 15645.

[17] Deposition Numbers 2044604 (**5b**), 2044605 (**5av**), 2044607 (**5bh**), and 2044608 (**(PhPhCOOBcat)$_2$·Ni(OOCPhPh)$_2$**) contain the supplementary crystallographic data for this paper. These data are provided free of charge by the joint Cambridge Crystallographic Data Centre and Fachinformationszentrum Karlsruhe Access Structures service www.ccdc.cam.ac.uk/structures.

[18] a) M. Murata, T. Oyama, S. Watanabe, Y. Masuda, *J. Org. Chem.* **2000**, *65*, 164 – 168; b) D. Mazzarella, G. Magagnano, B. Schweitzer-Chaput, P. Melchiorre, *ACS Catal.* **2019**, *9*, 5876 – 5880.

[19] a) K. Nakamura, M. Tobisu, N. Chatani, *Org. Lett.* **2015**, *17*, 6142 – 6145; b) C. Zarate, R. Manzano, R. Martin, *J. Am. Chem. Soc.* **2015**, *137*, 6754 – 6757; c) M. Tobisu, J. Zhao, H. Kinuta, T. Furukawa, T. Igarashi, N. Chatani, *Adv. Synth. Catal.* **2016**, *358*, 2417 – 2421; d) X.-W. Liu, J. Echavarren, C. Zarate, R. Martin, *J. Am. Chem. Soc.* **2015**, *137*, 12470 – 12473; e) T. Niwa, H. Ochiai, Y. Watanabe, T. Hosoya, *J. Am. Chem. Soc.* **2015**, *137*, 14313 – 14318; f) J. Zhou, M. W. Kuntze-Fechner, R. Bertermann, U. S. D. Paul, J. H. J. Berthel, A. Friedrich, Z. Du, T. B. Marder, U. Radius, *J. Am. Chem. Soc.* **2016**, *138*, 5250 – 5253; g) A. M. Mfuh, J. D. Doyle, B. Chhetri, H. D. Arman, O. V. Larionov, *J. Am. Chem. Soc.* **2016**, *138*, 2985 – 2988; h) M. Tobisu, K. Nakamura, N. Chatani, *J. Am. Chem. Soc.* **2014**, *136*, 5587 – 5590.

[20] J. Hu, M. Wang, X. Pu, Z. Shi, *Nat. Commun.* **2017**, *8*, 14993.

[21] Z. Zhang, P. Jain, J. C. Antilla, *Angew. Chem. Int. Ed.* **2011**, *50*, 10961 – 10964; *Angew. Chem.* **2011**, *123*, 11153 – 11156.

[22] a) G. R. Eaton, *J. Chem. Educ.* **1969**, *46*, 547 – 556; b) S. Hermanek, *Chem. Rev.* **1992**, *92*, 325 – 362.

[23] The actual transition state could be somewhat lower in energy due to possible intermolecular interactions, hydrogen bonding included.

[24] C. Kleeberg, L. Dang, Z. Lin, T. B. Marder, *Angew. Chem. Int. Ed.* **2009**, *48*, 5350 – 5354; *Angew. Chem.* **2009**, *121*, 5454 – 5458.

[25] a) P. R. McCarren, P. Liu, P. H. Cheong, T. F. Jamison, K. N. Houk, *J. Am. Chem. Soc.* **2009**, *131*, 6654 – 6655; b) T. Wititsuwannakul, Y. Tantirungrotechai, P. Surawatanawong, *ACS Catal.* **2016**, *6*, 1477 – 1486.

[26] X. Hong, Y. Liang, K. N. Houk, *J. Am. Chem. Soc.* **2014**, *136*, 2017 – 2025.

Manuscript received: May 11, 2021
Revised manuscript received: July 5, 2021
Accepted manuscript online: July 7, 2021
Version of record online: ■■ ■■, ■■■■

Research Articles

Nickel Catalysis

X. Deng, J. Guo, X. Zhang, X. Wang,*
W. Su* ——— ■■■■–■■■■

Activation of Aryl Carboxylic Acids by Diboron Reagents towards Nickel-Catalyzed Direct Decarbonylative Borylation

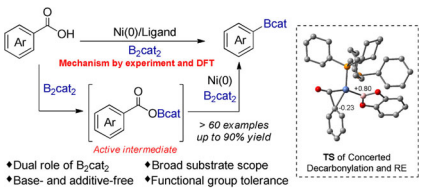

A Ni-catalyzed direct decarbonylative borylation of aryl carboxylic acids with B_2cat_2 has been established. B_2cat_2 serves as a borylating agent, but also activates the carboxylic acid substrate towards decarbonylative coupling, playing a dual role in this reaction. A combination of experimental and computational studies reveals that the reaction proceeds through a hitherto unknown concerted decarbonylation and reductive elimination step.